Int. J. Electrochem. Sci., 7 **(2012)** 12610 - 12620

International Journal of
ELECTROCHEMICAL
SCIENCE
www.electrochemsci.org

Corrosion Inhibition by a Coconut Oil Modified Imidazoline for Carbon Steel Under the Combined Effect of CO_2 and H_2S

L.M. Rivera-Grau[1], *M. Casales*[2], *I. Regla*[2,3], *D. M. Ortega-Toledo*[2],*D. Cuervo*[4], *J. Asencio*[4], *J.G. Gonzalez-Rodriguez*[1*], *L. Martine-Gomez*[2,4]

[1] Universidad Autonoma del Estado de Morelos, CIICAp, AV. Universidad 1001, 62209-Cuernavaca, Mor., Mexico
[2] Universidad Nacional Autonoma de Mexico, Instituto de Ciencias Fisicas, AV. Universidad s/n, Cuernavaca, Mor., Mexico
[3] Universidad Nacional Autonoma de Mexico, Facultad de Estudios Superiores Zaragoza, Mexico D.F., Mexico
[4]Corrosion y Proteccion, Rio Nazas 6, Cuernavaca, Morelos, Mexico
[*]E-mail: ggonzalez@uaem.mx

Received: 23 October 2012 / *Accepted:* 17 November 2012 / *Published:* 1 December 2012

A coconut-oil modified hydroxyetyl-imidazoline has been synthesized and used as a carbon dioxide + hydrogen sulfide corrosion for carbon steel in 3% NaCl solution at 50°C. Testing techniques includes potentiodynamic polarization curves, linear polarization resistance, and electrochemical impedance spectroscopy. Results indicated that with only 20 ppm the coconut oil-modified inhibitor acted as an effective corrosion inhibitor for carbon steel in presence of both carbon dioxide +hydrogen sulfide, reaching efficiency values as high as 97, which is very encouraging for the preparation of green corrosion inhibitors.

Keywords: Green inhibitor, carbon steel, acidic corrosion.

1. INTRODUCTION

It is well known that the carbon dioxide corrosion of carbon steel is a key problem in the gas and oil industry. Recently, carbon dioxide corrosion becomes even more serious along with increasing the carbon dioxide and water in oil field as result of exploration in middle or later period and using the technique of enhanced oil recovery. Several mechanisms have been provided to interpret the mechanism of the carbon dioxide corrosion of carbon steel [1-3]. During these corrosion processes, the carbon steel surface can be covered by an iron carbonate corrosion scale which could slow down the corrosion rate and could protect the substrate from further corrosion [4-6]. The tubing steel may be not

only suffered from carbon dioxide corrosion, but also suffered from different stress states underground, moreover, the stratum water may contain some aggressive anions, i.e., sulfur ions and chloride ions. Though so much effort has been taken on the carbon dioxide corrosion or hydrogen sulfide corrosion, little attention was paid on the corrosion in the oil and gas well where carbon dioxide and hydrogen sulfide coexist. For instance, Ren et al. [6] used electrochemical measurement techniques, X-ray diffraction and scanning electron microscopy to investigate the corrosion behavior of N80 tube steel in a chloride-containing solution with carbon dioxide and hydrogen sulfide at a temperature of 100 ◦C. Sweet corrosion occurred when a very small partial pressure of hydrogen sulfide was added. At this condition, uniform corrosion was found. The added hydrogen sulfide only accelerated the general corrosion rate. Sour corrosion was primary as the partial pressure of hydrogen sulfide increased to 0.010MPa. The general corrosion rate decreased quickly, but severe pitting was found. The injection of corrosion inhibitor is a standard practice in oil and gas production systems to control internal corrosion of carbon steel structures. Nitrogen-based organic inhibitors, such as imidazolines or their salts have been successfully used in these applications even without an understanding of the inhibition mechanism [7-14]. The corrosion inhibition of organic compounds is related to their adsorption properties. Adsorption depends on the nature and the state of the metal surface, on the type of corrosive environment and on the chemical structure of the inhibitor [13]. Different derivatives from imidazolines are employed as steel corrosion inhibitors. Recently Yoo et al. [15] evaluated a bio-diesel-based imidazoline, namely 2-(2-alkyl-4,5-dihydro-1H-imidazol-1-yl)ethanol, as corrosion inhibitor of mild steel in 1.0 M hydrochloric acid and compared with the same imidazoline but prepared with petroleum-based chemicals. It was found that when the bio-diesel-based imidazoline had a concentration over 100 ppm, it acted as an effective corrosion inhibitor. An undergoing research project in our laboratory deals with the possibility of using coconut oil as corrosion inhibitors. Thus, the aim of this work is to evaluate the corrosion inhibition performance of a coco-modified imidazoline in an carbon dioxide +hydrogen sulfide corrosion-containing environment.

2. EXPERIMENTAL

Material tested was a 1018 carbon steel cylinder measuring 25 mm in length and 5.0 mm diameter. Before testing, the electrode was polished to 600 grit SiC emery paper and then cleaned with alcohol, acetone and distilled water. Inhibitor used in this work includes a commercial hydroxyetyl-imidazoline which has been modified with coconut oil as follows. A mixture of distilled coconut biodiesel (59-120 °C/0.05 mmHg) 2.22 g and 0.936 g of 2-(2-aminoethylamino)ethanol were heated and magnetically stirred at 140 ° C during 9 hours at atmospheric pressure and 3 hours at a reduced pressure (20 mm Hg). The reaction mixture was distilled at the Kugelrohr apparatus under reduced pressure (235 °C /0.05 mmHg) to obtain 1.42 g of coconut imidazoline mixture. Inhibitors were dissolved in pure 2-propanol. The general structure of both inhibitors is shown on Fig. 1. The concentration of the inhibitor used in this work was 25 ppm and the temperature kept at 50°C. Testing solution consists of 3% sodium chloride solution, heated, de-aerated by purging with carbon dioxide gas during 2 hours prior the experiment and kept bubbling throughout the experiment. Hydrogen

sulfide was produced by reacting sodium sulfide with acetic acid. Inhibitor is added 2 hours after pre-corroding the specimens in the solution. Electrochemical techniques employed included potenthiodynamic polarization curves, linear polarization resistance, LPR, and electrochemical impedance spectroscopy, EIS.

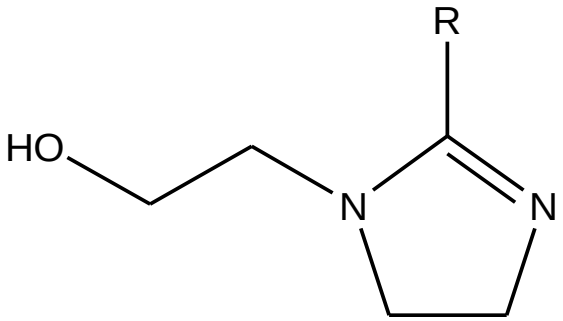

Figure 1. General structure of hydroxyethyl imidazoline, where R is an alkyl chain derivative.

Polarization curves were recorded at a constant sweep rate of 1 mV/s and the scanning range was from -300 to +300 mV respect to the open circuit potential, E_{corr}. Measurements were obtained by using a conventional three electrodes glass cell with two graphite electrodes symmetrically distributed and a saturated calomel electrode (SCE) as reference with a Lugging capillary bridge.

LPR measurements were carried out by polarizing the specimen from +10 to –10 mV respect to E_{corr}, at a scanning rate of 1 mV/s. Inhibition efficiencies [*E(%)]* were determined according to the following equation:

$$E(\%) = \frac{R_{p,i} - R_{p,b}}{R_{p,i}} \text{ X } 100 \qquad (1)$$

where $R_{p,b}$ is the linear polarization resistance without inhibitor and $R_{p,i}$ is the linear polarization resistance with inhibitor. Electrochemical impedance spectroscopy tests were carried out at E_{corr} by using a signal with an amplitude of 10 mV and a frequency interval of 0.1-100KHz. An ACM potentiostat controlled by a desk top computer was used for the LPR tests and polarization curves, whereas for the EIS measurements, a model PC4 300 Gamry potentiostat was used.

3. RESULTS AND DISCUSSION

The effect of inhibitor in the polarization curve for carbon steel in the sodium chloride solution with addition of carbon dioxide +hydrogen sulfide is shown in Fig. 2, where can be seen that the highest corrosion current density value, i_{corr}, is shown when carbon dioxide alone is added to the sodium chloride solution, followed by the later solution. In all cases, the polarization curves did not show the presence of a passive layer, only anodic dissolution, with an increase in the anodic current

density as the anodic potential increases. However, when hydrogen sulfide is added to the sodium chloride solution, the i_{corr} value is decreased for almost one order of magnitude, showing an inhibitive effect of hydrogen sulfide under some conditions as reported by Wang [12] and Farelas [13] which is due to the formation of a protective, stable iron sulfide film on the steel surface. On the other hand, in presence of carbon dioxide, iron and steel form an iron carbonate film.

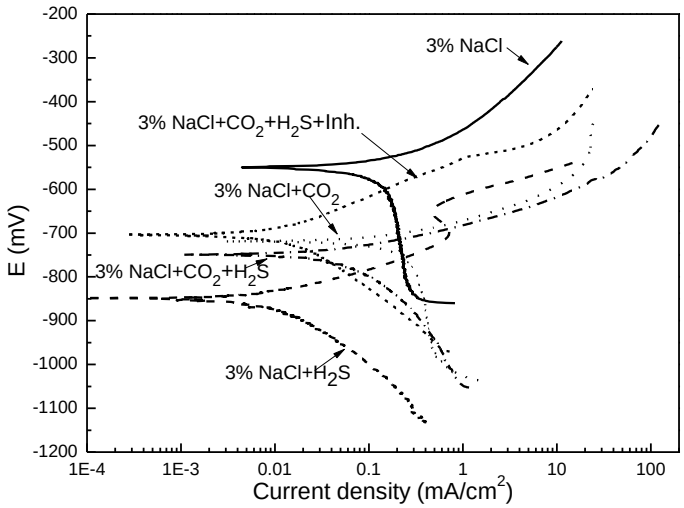

Figure 2. Effect of inhibitor on the polarization curves in the H_2S and CO_2-containing 3% NaCl solution at 50°C.

Table 1. Electrochemical parameters obtained from polarization curves.

Solution	E_{corr} (mV_{SCE})	i_{corr} (mA/cm^2)	b_a (mV/dec)	b_c (mV/dec)
3% NaCl	-552	0.16	60	856
3% NaCl+ CO_2	-720	0.31	60	720
3% NaCl+ H_2S	-850	0.015	50	150
3% NaCl+ +CO_2+ H_2S	-750	0.07	40	190
3% NaCl+ CO_2+ H_2S+ Inh.	-620	0.014	85	170

When both carbon dioxide and hydrogen sulfide were added, the corrosion current density was higher than that obtained in presence of carbon dioxide alone but lower than that with the addition of hydrogen sulfide, showing the competitive effect of both ions. Finally, when the coconut oil-modified imidazoline is added in presence of both carbon dioxide and hydrogen sulfide the steel showed a corrosion rate very similar to that found in presence of hydrogen sulfide only, indicating apparently that the inhibitor was not acting on the steel surface. Electrochemical parameters found from these polarization curves are shown in table 1. A cathodic limiting current density value can be seen for the

sodium chloride solution and in presence of carbon dioxide which is due to its hydration to give carbonic acid as follows [16]:

$$CO_2 + H_2O \rightarrow H_2CO_3 \quad (2)$$

Since the solution is de-aerated, the dominant cathodic reactions are the reduction of H^+ ions, dissociation of carbonic acid [17-19]:

$$H_2CO_3 + e^- \rightarrow H^+ + HCO_3^- \quad (3)$$

$$HCO_3^- + e^- \rightarrow H^+ + CO_3^{2-} \quad (4)$$

$$2H^+ + 2e^- \rightarrow H_2 \quad (5)$$

and water reduction:

$$2H_2O + 2e^- \rightarrow 2OH^- + H_2 \quad (6)$$

The main anodic reaction, in absence of inhibitor, is iron dissolution according to:

$$Fe \rightarrow Fe^{2+} + 2e^- \quad (7)$$

though it may be through several steps. During this corrosion process, a corrosion scale of iron carbonate would form on the surface of carbon steels according to [20]:

$$Fe^{2+} + CO_3^{2-} \rightarrow FeCO_3 \quad (8)$$

On the other hand, in presence of hydrogen sulfide the cathodic reaction that occurs is:

$$H_2S_{(aq)} + 2e^- \rightarrow S^{2-} + H_2 \quad (9)$$

using the electrons coming from anodic reaction (7) giving as na overall reaction the formation of iron sulfide film according to:

$$Fe + H_2S_{(aq)} \rightarrow \square FeS + H_2 \quad (10)$$

In order to have a better insight on the inhibitor performance on the steel surface in presence of the combination of carbon dioxide + hydrogen sulfide, some linear polarization resistance measurements were undertaken during 24 hours, and the results are shown in Fig. 3. This figure confirms the results found in the polarization curves: the acceleration in the corrosion rate with the

addition of carbon dioxide, since the polarization resistance value, R_p, found with its addition was lower than that found for sodium chloride solution, and the inhibitive effect of the addition of hydrogen sulfide, since the R_p value found with its addition was higher than that for sodium chloride solution. On the other hand, the R_p value for the solution with the addition of both carbon dioxide + hydrogen sulfide showed intermediate values between the respective values found in presence of either carbon dioxide or hydrogen sulfide alone. However, when the coconut oil-based inhibitor is added, the R_p value increased as time elapsed reaching values almost one order of magnitude that the uninhibited solution in presence of both aggressive ions.

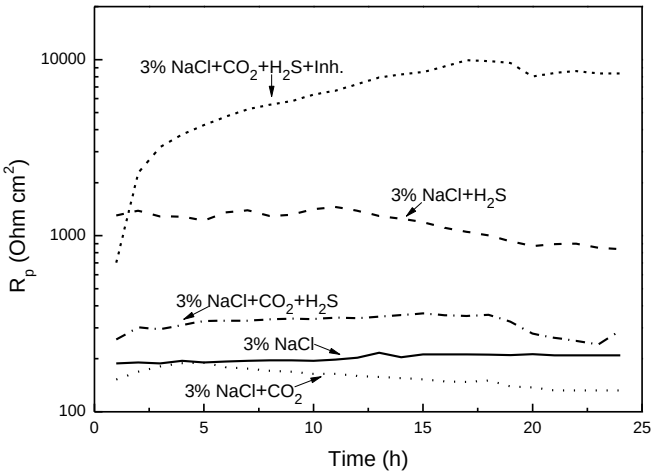

Figure 3. Effect of inhibitor on the change of the R_p value with time in the H_2S and CO_2-containing 3% NaCl solution at 50°C.

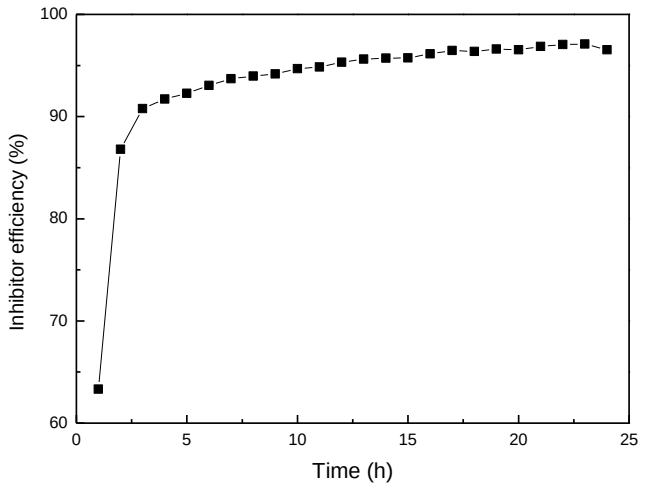

Figure 4. Change in the inhibitor efficiency with time for carbon steel exposed to a 3% NaCl solution containing CO_2 and H_2S at 50°C.

The fact that the R_p value for the solution containing only either carbon dioxide or hydrogen sulfide decreases with time indicates the unstability of the film formed under the steel surface in each case. On the other hand, the fact that the R_p value in presence of the inhibitor, shows that the film formed in this cases is very stable and protective. The inhibitor efficiency values calculated by using eq. (1) are shown in Fig. 4, where it can be seen that vales as high as 97 % are reached. This fact shows the good inhibitory effect of this vegetable oil-based inhibitor.

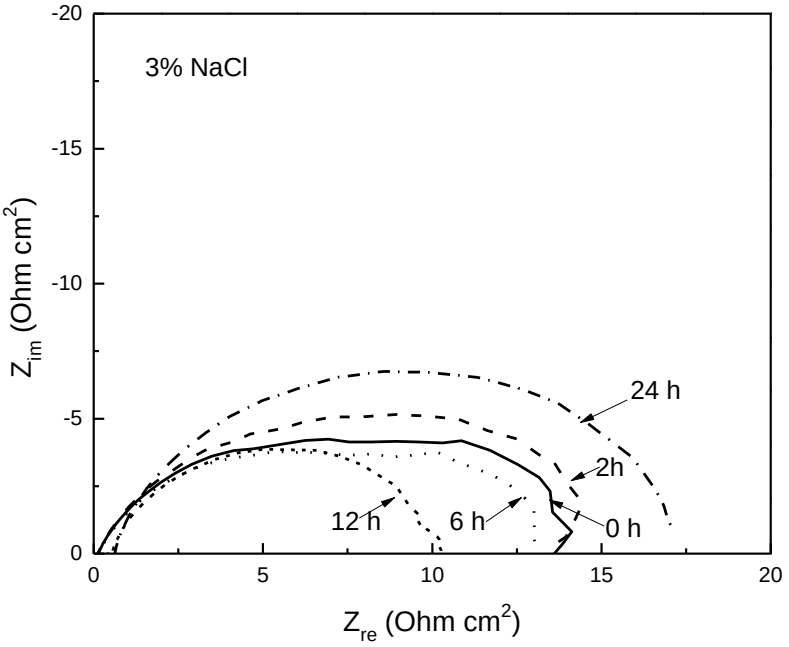

Figure 5. Nyquist diagrams for carbon steel exposed to a 3% NaCl solution at 50°C.

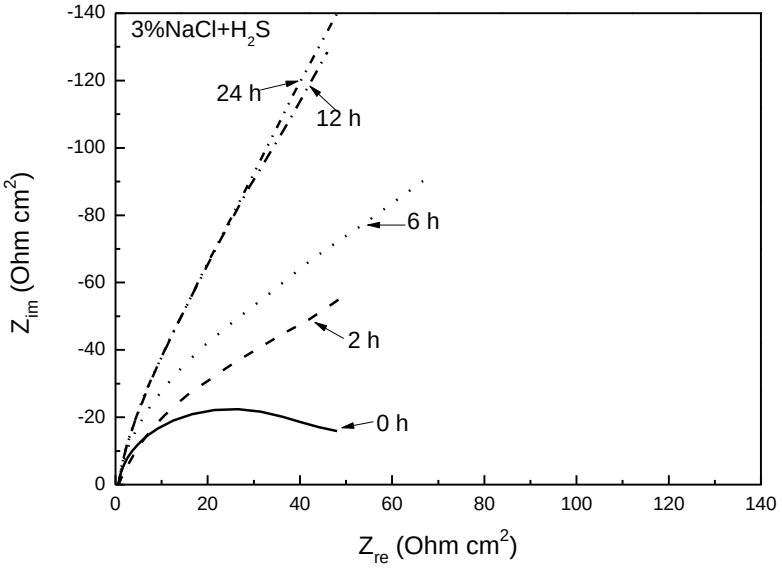

Figure 6. Nyquist diagrams for carbon steel exposed to a 3% NaCl + H_2S solution at 50°C.

Niquist diagrams for the 3% sodium chloride solution during the 24 hours of testing are shown in Fig. 5 which shows at all times depressed capacitive-like semicircles, with their centers in the real axis, indicating that the corrosion process is under charge transfer control from the metal to the electrolyte through the double electrochemical layer.

The semicircle diameter practically remained the same throughout the test, around 15 ohm cm^2. However, when hydrogen sulfide was added to the solution, Fig. 6, the semicircle diameter was higher than that obtained with pure sodium chloride solution, obtaining its lowest value at the beginning of the experiment, around 50 ohm $cm^2$and kept increasing as time elapsed reaching its highest value after 24 hours of testing.

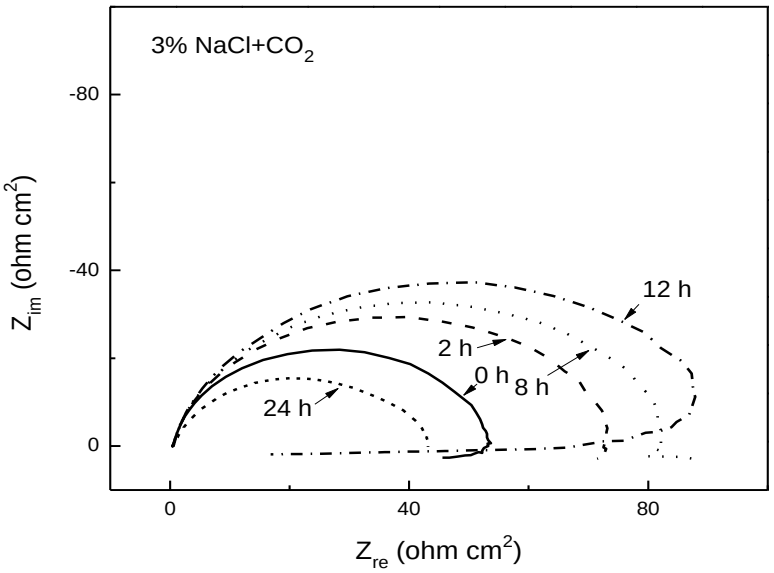

Figure 7. Nyquist diagrams for carbon steel exposed to a CO_2-saturated 3% NaCl solution at 50°C.

Nyquist diagram for carbon steel exposed to a carbon dioxide-saturated 3% sodium chloride solution at 50 °C is shown on Fig. 7, where it can be seen that the data describe a depressed, capacitive-like semicircle at high and intermediate frequency values, followed by an inductive semicircle at lower frequency values, especially at 0 and 12 hours, indicating that the corrosion process is controlled by some intermediate species. The appearance of the inductive loop in the Nyquist plots is attributed to the adsorption of an intermediate product in the corrosion reaction. This is consistent with the proposed involvement of adsorbed intermediates in the anodic dissolution of iron in acidic solution by Bockris et al. [22] in carbon dioxide saturated solutions [23] and has been established to be adsorbed iron hydroxide. Sometimes, the inductive semicircle does not exist only a single depressed, capacive-like one. The semicircle diameter corresponds to the charge transfer resistance, R_{ct}, equivalent to the polarization resistance, R_p, thus inversely proportional to the corrosion current density, i_{corr} . As time elapses, the semicircle diameter increases but after 12 hours it decreases, increasing, thus, the corrosion rate, showing the non-protective nature of the corrosion products.

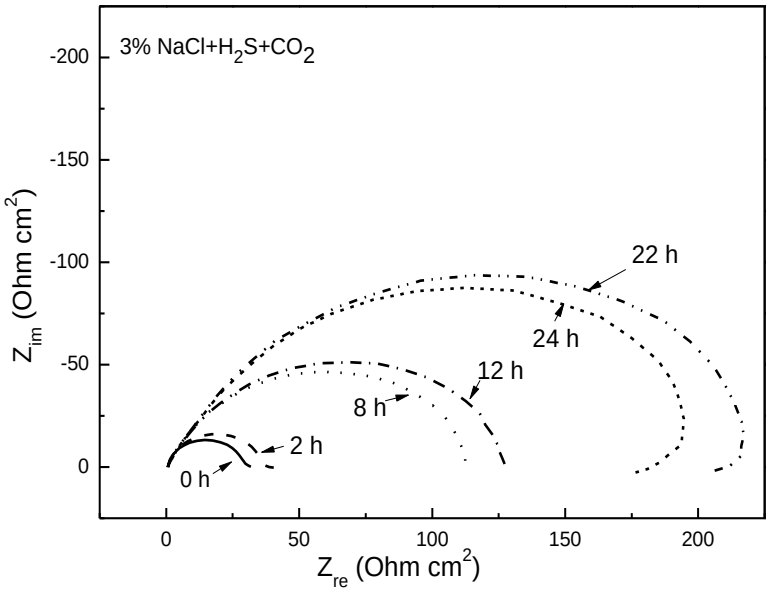

Figure 8. Nyquist diagrams for carbon steel exposed to a 3% NaCl solution containing CO_2 and H_2S at 50°C.

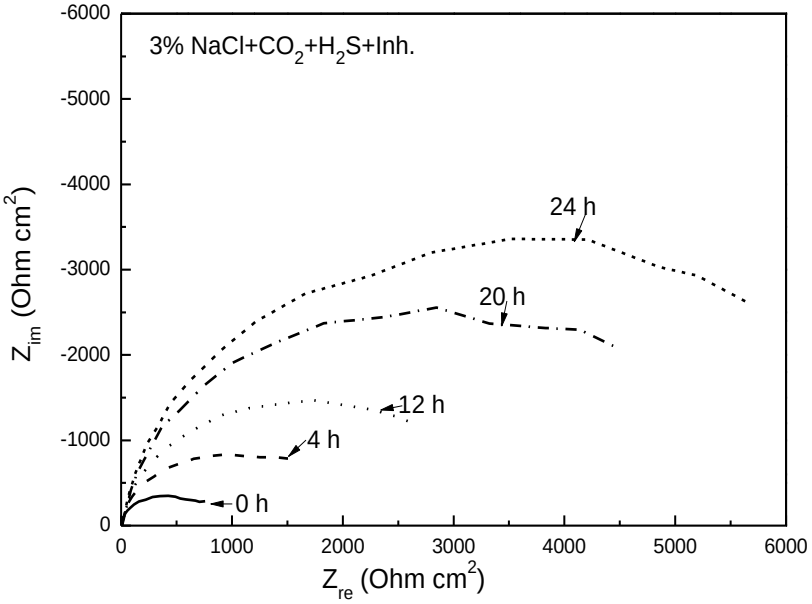

Figure 9. Nyquist diagrams for carbon steel exposed to a 3% NaCl solution containing CO_2 , H_2S and inhibitor at 50°C.

When both carbon dioxide and hydrogen sulfide are present, Fig. 8, Nyquist diagram consist of a single depressed, capacive-like semicircle with its centre in the real axis during the first 12 hours or so, indicating that the corrosion process is controlled by the charge transfer from the metal to the electrolyte through the double electrochemical layer, whereas at longer times, data consist of a depressed, capacitive-like semicircle at high and intermediate frequency values, followed by an

inductive semicircle at lower frequency values, indicating that the corrosion process is controlled by some intermediate species. The semicircle diameters were higher than those obtained with the addition of only carbon dioxide. Finally, when the inhibitor is added to the solution containing carbon dioxide and hydrogen sulfide, Fig. 9, Nyquist diagrams showed one capacitive loop at high frequency and a straight line or what appears to be an incomplete semicircle at lower frequency values at short times, although for longer times the second semicircle present at lower frequency values is more obvious. The first, high frequency, semicircle is due to the double electrochemical layer, whereas the second, lower frequency semicircle is due to the presence of a protective film due to the corrosion products and the inhibitor. As time elapses, the semicircle diameter increases, more than one order of magnitude higher than that obtained for the uninhibited solution, indicating that the film-formed inhibitor is very stable.

Thus, it is obvious that when carbon dioxide is added to the sodium chloride solution the corrosion rate of carbon steel increases as compared to that obtained in pure sodium chloride and the formed iron carbonate film is non-protective. On the other hand, when hydrogen sulfide is added to the sodium chloride solution, it has an inhibitive effect since the corrosion rate of carbon steel decreases as compared to that obtained in pure sodium chloride solution and the formed iron sulfide film is more protective than iron carbonate. However, as shown by the LPR results in Fig. 3, the R_p value decreases with time, indicating that iron sulfide film is not stable with time. When both carbon dioxide and hydrogen sulfide are added to the sodium chloride solution, the corrosion rate of carbon steel is lower than that obtained when only carbon dioxide is added but higher than that obtained with the addition of only hydrogen sulfide, i.e. there seems to be a competitive effect between both gases. When the inhibitor is added in presence of both carbon dioxide and hydrogen sulfide, the film formed by the inhibitor, is protective and very stable with time as shown in Figs. 3 and 8, since the R_p value continuously increases as time elapses. This effect has been explained in terms of the inhibitor molecular structure, since the molecular structure of hydroxyethyl imidazoline, Fig. 1, is composed of a five member ring containing nitrogen elements, a C-14 saturated hydrophobic head group and a pendant, hydrophilic hydroxyethyl group attached to one of the nitrogen atoms. The compound can be adsorbed on the metal surface by the formation of an iron-nitrogen co-ordination bond and by a pi-electron interaction between the pi-electron in the head group and iron [10-12]. Though not a primary contribution to the adsorption strength of the compound on the surface of the metal, coulombic attraction between the negative charge, i.e. electrons, on the metal surface (as a result of the specific adsorption of chloride ions) and the imidazoline derivative may also contribute to the inhibition ability of the compound. When the adsorbed inhibitor molecules exceed certain number of atoms on the surface and these molecules are close enough, electrostatic repulsion between the negative charge of the pendant group, leads to a desorption of the inhibitor molecules, leading to unprotected sites on the metal and an increase on the corrosion rate. The fact that the coconut-modified imidazoline has an excellent corrosion inhibitor performance is very encouraging because provides very promising results in the preparation of green corrosion inhibitors.

4. CONCLUSIONS

The corrosion inhibition performance of a coconut-oil modified imidazoline for carbon steel exposed to both carbon dioxide and hydrogen sulfide in 3% sodium chloride solution at 50°C has been evaluated. All the different techniques have shown that very small amounts of this vegetable-based inhibitor, 20 ppm, can be very efficient in decreasing the degradation rate of carbon steel in such as aggressive conditions, forming a very stable stable, protective film. These results provide very promising results in the preparation of green corrosion inhibitors.

References

1. M. B. Kermani, A. Morshed, *Corrosion* 59 (2003) 659.
2. K. Videm, J. Kvarekval, *Corrosion* 51 (1995) 260.
3. T. Hong, Y. H. Sun, W. P. Jepson, *Corros. Sci.* 44 (2002) 101.
4. D. A. Lopez, W. H. Schreiner, S. R. de Sanchez, S. N. Simison, *Appl. Surf. Sci.* 207 (2003) 69
5. S. L.Wu, A. D.Cui. F. He, Z. Q. Bai, S. L. Zhu, X. J. Yang, *Materials Letters* 58 (2004) 1076.
6. C. Ren, D. Liu, Z. Bai, T. Li, *Mat. Chem. Phys*. 93 (2005) 305.
7. J. B. Li, X. Hou, M.S Zheng, J. W. Zhu, *Int. J. Electrochem. Sci*. 2 (2007) 607.
8. Ramachandran S, Jovancicevic V., *Corrosion* 55 (1999) 259.
9. Z. Xueyuan, *Corros. Sci*. 43 (2001) 1417.
10. F. Bentiss, M. Lagrenee, M. Traisnel, J.C. Hornez, *Corros. Sci.* 41 (1999) 789.
11. S. Ramachandran, M. Tsai, M. Blanco, H. Chen, W. A. Tang, Godard III, *Langmuir* 12 (1996) 6419.
12. D. Wang, S. Li, M. Ying, M. Wang, Z. Xiao, Z. Chen, *Corros. Sci*, 41 (1999) 1911.
13. F. Farelas, A. Ramirez, *Int. J. Electrochem. Sci*. 5 (2010) 797.
14. Lijuan Feng, Huaiyu Yang, Fuhui Wang, *Int. J. Electrochem. Sci*. 7 (2012) 4064.
15. S.H. Yoo, Y. W. Kim, K. W. Chung, S. Y. Baik, J. S. Kim, *Corros. Sci*. 59 (2012) 42.
16. K.G. Gonroy, C.B. Breslin, *Electrochim. Acta* 48 (2003) 721.
17. S. Arzola, J. Mendoza-Florez, R. Duran-Romero, J. Genesca, *Corrosion*, 62 (2006) 433.
18. P.H. Tewart, A.B. Campbell, *Can. J. Chem*. 57 1979) 188.
19. F.H. Meyer, O.L. Riggs, R.L. McGlasson, J.D. Sudbury, *Corrosion* 14 (1958) 69.
20. G.W. Walter, *Corros. Sci*. 26 (1989) 681
21. K. Hladky, J.L. Dawson, *Corros. Sci*. 22 (1982) 231.
22. J.O.M. Bockris, D. Drazic, A.R. Despic, *Electrochim. Acta* 4 (1961) 325.
23. F. Bentiss, M. Traisnel, M. Lagrenée, *J. Appl. Electrochem*. 31 (2001) 41.